Microchemical Journal 164 (2021) 105923

Contents lists available at ScienceDirect

Microchemical Journal

journal homepage: www.elsevier.com/locate/microc

Sensitive fluorometric determination of gold in geological samples using fire assay pre-concentration coupled with microfluidic paper-based analytical device

Akram Hajinia, Tahereh Heidari *

Department of Chemistry, Faculty of Sciences, Ferdowsi University of Mashhad, Mashhad, Iran

ARTICLE INFO

Keywords:
Paper-based device
Microfluidics
Gold
Fluorimetry
Smart phone
Image analysis

ABSTRACT

The present study was conducted to develop a simple, low-cost and sensitive micro fluidic paper-based analytical device (μPAD) for analysis of gold in geological samples. This μPAD was fabricated employing eyeliner pencil method. It consists of different zones, including detection, pH adjustment, reaction and elution. We injected 29 μL elution solution in the center of μPAD, direct Au^{3+}, after adjusting pH, to make it react with rhodamine B. The formation of RB-Au^{3+} complex led to quench of rhodamine B fluorescence. The image of each detection zone was captured using a cell phone camera under a UV lamp, and luminosity intensity was subsequently measured with Photoshop software. Various parameters were studied in order to achieve the most efficient performance of the paper sensor. Under the optimized condition, a wide linear range (1–40 mg L^{-1}, $R^2 = 0.996$) was obtained with detection limit of 0.15 mg L^{-1}. Ultimately, the developed μPAD was applied for the determination of gold in ore samples. The obtained results were in good agreement with those obtained from standard method. The combination of fire assay and μPAD in the determination of gold in geological samples improved the detection limit based on enrichment factor of 75.

1. Introduction

Quantification of gold in trace levels is of great importance in geosciences and mining industry. It is widely applied in electronic gadgets, medicine, jewelry and manufacturing of currencies [1]. Low abundance of gold and high salt content in rock and ore samples make serious limitations in the direct determination of gold [2]. Therefore, to improve the level of detection and selectivity, several separation and preconcentration methods have been developed, such as lead/nickel sulfide fire assay [3], solvent extraction [4,5], co-precipitation [6], ion-exchange [7] and adsorption [8]. Among these techniques, fire assay is still considered as the reference method. This method is combined with atomic absorption spectrometry (AAS) or inductively coupled plasma atomic emission spectroscopy (ICP-AES) [9–12].

Microfluidic Paper-based analytical devices (μPADs) are patterns containing hydrophilic channels and hydrophobic walls [13,14]. Capillary action in the porous network of paper, transports solution through the channels without any external source [15,16]. Wax printing [17–20], inkjet printing [21], photolithography [22,23], flexographic printing, plasma treatment [24], laser treatment [25], sol-jell method [26,27], screen-printing [28], and wax screen-printing[11] are various ways applied for preparing patterned papers [29,30]. Colorimetry [31,32], electrochemistry [33,34], fluorescence [35,36], chemiluminescence (CL) [37,38], electrochemiluninescence (ECL) [39,40], photoelectrochemistry (PEC) are different detection methods in this technique [41]. Paper-based analytical devices using fluorescent reagents have attracted a great deal of attention owing to their high sensitivity and selectivity, and that they do not require any expensive instruments [42]. Nowadays, the collected samples from mines are transported to some laboratories for gold analysis. Following fire assay pre-concentration, several instrumental techniques are applied to measure gold, particularly atomic absorption spectroscopy and inductively couple plasma spectrometry. These equipment are expensive, need skillful operators and are not easily accessible in developing countries. Consequently, there is a requirement for sensitive and low-cost methods for gold determination. Fire assay pre-concentrates gold and eliminates matrix of ores. On the other hand, μPAD is cheap, easy to operate and consumes small sample volumes [43]. This research demonstrated for the first time, a low-cost, selective and sensitive method for quantification of gold in ores, in combination of fire assay and μPAD. The device

* Corresponding author.
E-mail address: taherehheidari@um.ac.ir (T. Heidari).

https://doi.org/10.1016/j.microc.2021.105923
Received 23 May 2020; Received in revised form 31 December 2020; Accepted 2 January 2021
Available online 6 January 2021

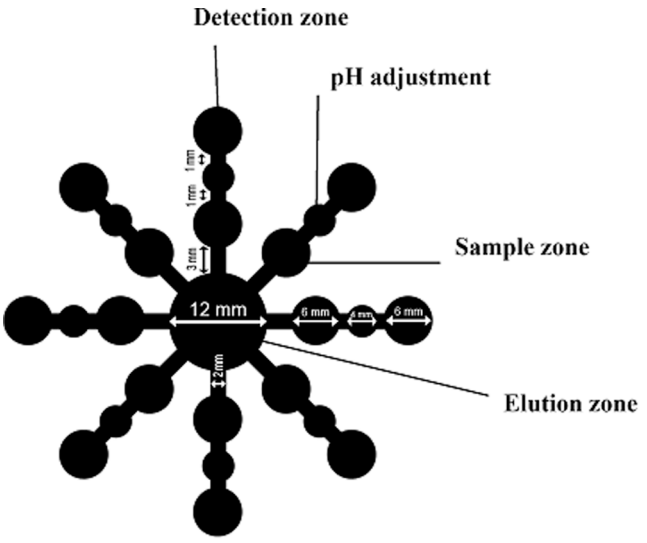

Fig. 1. Design of μPAD petal-like shape.

consists of reaction, detection, pH adjustment and elution zones. Employing this device, after loading of set volumes of standard and reagent solutions, pipetting of elution solution in the center of device, Au+3, is moved to pH adjustment zone, then reacts with rhodamine B (RB). The concentration of gold in samples is quantified by determining fluorescence quenching of rhodamine B on the μPAD. Luminosity under UV lamp, is directly proportional to the log Au3+ concentration.

2. Experimental

2.1. Materials and apparatus

The utilized apparatuses included disk mill (RS-100 (Retsch, Germany)), analytical balance (Sartorius, Germany), muffle furnace (0–1200 °C) (Iran Khodsaz, Iran), atomic absorption spectrophotometer (NOVA400 (Analytik Jena, Germany), spectrofluorometer (Synergy H4 microplate reader (Bio Tek,USA), cellphone (iPhone 7 s), micropipettes (Eppendorf 0-2μlit and Brand 10,100,1000 μlit), filter paper (Whatman NO 40,41,42), eye pencil (Bourjois, France), hot plate (Alfa, Tehran, Iran), homemade light control box (35 × 25 × 25 cm) and UV lamp (Noor,Tehran, Iran).

All the chemicals employed in this research were on analytical grade. The solutions and samples were prepared in deionized water. Standard gold solution (1000 mg L^{-1}), rhodamine B, sodium chloride, sodium hydroxide, nitric and hydrochloric acid were purchased from Merck (Germany). A solution of rhodamine B was prepared dissolving 0.0018 g of rhodamine B in 10 mL of deionized water. Gold certificated reference materials (CRMs) (OXL78, OXJ95, OXE106, OXC129, SH82) and (OREAS 250) were used from ROCKLABs and OREAS companies, respectively.

2.2. Design and fabrication of μPAD

The microfluidic platform was fabricated using the eyeliner pencil method [44]. Initially, the petal-like shape was designed in AutoCAD 2014 (Fig. 1). It had 8 branches consisting of detection (Ø = 6mm), pH adjustment (Ø = 4mm), sample or standard reservoirs (Ø = 6mm) and elution zone (Ø = 12 mm). Subsequently, this pattern was cut on a sticker with a CO_2 laser. Afterwards, the hydrophobic barriers were formed on the whatman NO.41, according to the previously reported procedure [44]. Varying of volumes of RB and sample solutions (0.4–1.4 μL) were dropped in the detection and sample zones. We selected the sample volume necessary to wet the entire sample and detection zones without spreading out therefore, we determined 1.2 μL of sample solution and 0.6 μL of indicator solution for the further experiments. It was found that 29 μL of elution solution was required to fill all detection zones.

2.3. Fire assay pre-concentration procedure

The gold content of ores and rocks is commonly determined by lead-fire assay method. 50 g of pulverized sample was melted in a mixture of 150 g flux containing flour, lead oxide, soda, borax, and silica in a furnace at temperatures between 900 °c and 1100 °c. The lead oxide was then reduced easily to metal form whereas collecting the gold, and this lead–gold alloy, after the cooling, was separated from slag. Then, it was re-melted in a bone-ash cupel, which absorbed the lead oxide formed but left a bead of gold-silver that was dissolved in 1 mL aqua regia for quantitative analysis [45].

2.4. Detection and image processing

1.2 μL of the standard or sample solutions were individually pipetted into the sample zones. 0.5 μL indicator solution was spotted into the detection reservoirs of μPAD (Fig. 1). The channels also contained pH adjustment zones. Impregnating the pH zones with 0.8 μL, NaOH(4 mol L^{-1}) samples' excess acid were neutralized. After drying in air, a polydimethylsiloxane (PDMS) lid with a hole punched over the elution zone was placed on top of the chip. Finally, 29 μL elution solution (NaCl 40 mmol L^{-1}) were pipetted into the central hole. It eluted analyte from sample zones to the detection zones. Once gold solution wicked rhodamine B, the reaction occurred and fluorescence quenching of rhodamine B was observed. μPAD was allowed to completely dry for 15–20 min at room temperature. In the end, the photo of μPAD was captured using an iPhone 7 s [46] in a light box under the exposure of a UV lamp. In order to obtain background-corrected data, the photos of μPAD were captured ahead of the deposition of elution solution (as the blank photo) and after pipetting the elution solution and reaching Au^{3+} to RB (as the analyte photo). Afterwards, the images were imported to Photoshop CS5 and the luminosity of sample to blank (L_{sample}/L_{blank}) was calculated. Obviously, the luminescence change could be observed with naked eye and used for semi qualification.

3. Results and discussions

3.1. Evaluation of fluorescence spectra

Fig. S1 demonstrates spectrofluorometric spectra of RB (0.016 mmol L^{-1}) and complex of Au^{+3}-RB (10 and 20 mg L^{-1} of Au^{3+}) at pH 3. The excitation wavelength was adjusted to 520 nm [47]. We observed the reaction between $AuCl_4^-$ ion and cationic form of RB forms, an association complex, and a decrease in the fluorescence intensity [48].

3.2. Optimization of μPAD features:

3.2.1. Effect of paper type

The metal complex must be uniformly spread over the detection zone to increase the accuracy and precision. Homogeneity and color intensity are highly dependent on pore size of the paper [49]; therefore, the most efficient paper should be selected for each work. A series of paper devices were fabricated using different types of papers. Whatman filter papers NO. 40, 41, 42 as well as office paper were evaluated in this study. As can be observed in Fig. S2, the similar results belong to whatman 41 and 40, which are of the largest pore size. Whatman NO 42 with a smaller pore size, does not have color uniformity. Non-porous office paper resisted against flow solution. Accordingly, whatman 41 was selected.

3.2.2. Investigation of the optimum color parameter

Photos of μPADs were taken with an iPhone7s in a homemade light

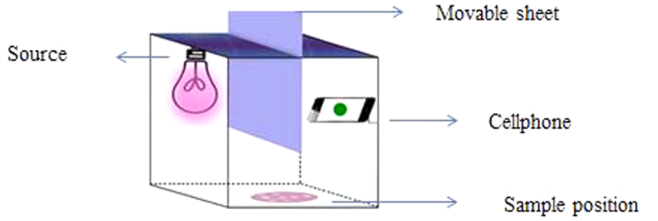

Fig. 2. Diagram of homemade light box (34 × 25 × 25 cm). Position of the source, cellphone and sample was fixed.

box, as shown in Fig. 2. The movable sheet in the box, between the source and the detector, prevented light from reaching the camera. To quantify the intensity of the color, Photoshop CS5 software was utilized. The appropriate detection zone of the platform was selected, and the mean intensity of all the colors was measured from histogram, as shown in Fig. S3. Luminosity intensity was used due to the steepest slope and a satisfactory R^2.

3.3. Optimization of affecting parameters for reaction between rhodamine B and Au^{3+}

3.3.1. Effect of rhodamine B concentration:

Herein, we evaluated the effects of Rhodamine B (RB) concentration, as a fluorometric reagent. In this investigation, μPAD was fabricated using 0.093, 0.125, 0.187, 0.253 and 0.375 mmol L^{-1} Rhodamine B on the detection zones and spotting 20 mg $L^{-1}Au^{3+}$ on the standard reservoirs. Fig. S4 illustrates that the concentration of 0.187 mmol L^{-1} of Rhodamine B provided the highest fluorescence quenching. Thus, this concentration was selected in the following experiments.

3.3.2. Effect of pH

To evaluate the effect of pH on the quenching of RB, pH of the solutions were adjusted in the range of 2–11 with HCl (0.1 mol L^{-1}) and NaOH (0.1 mol L^{-1}). As shown in Fig. S5, the highest fluorescence quenching effect belonged to acidic media (pH2-4), because in HCl media, RB forms an ion associate complex with gold (III) chloride [50] and at high pH other species, such as $AuOHCl_3^-$, $AuOH_2Cl_2^-$, $AuOH_3Cl^-$, $AuOH_4^-$ are formed [51]. $AuCl_4^-$ is more stable in acidic media and can sufficiently react. pH < 2 was not considered since they degraded or pierced the paper.

3.3.3. Effect of elution solution

Water and different concentrations of NaCl (10, 30, 40, 50 mmol L^{-1}) solutions were investigated and injected into the elution zones. Each plot was obtained by the analysis of intensity in Luminosity mode (Fig S6). The obtained data indicated that 30, 40 and 50 mmol L^{-1} NaCl was more effective on L_{sample}/L_{Blank}. Therefore, 40 $mmol^{-1}$ was selected for further experiments.

$AuCl_4^-$ reacted with the cationic form of the reagent to form an association complex; it is probable that the solution of salt improved this reaction and reduced fluorescence intensity.

3.4. Analytical figures of merit

3.4.1. Linear range and limit of detection

Under the optimized conditions, a linear calibration curve (log scale) was obtained in the range of 1–40 mg L^{-1} with $R^2 = 0.996$ (Fig. 3). The detection limit was obtained as 0.15 mg L^{-1} defined as a concentration

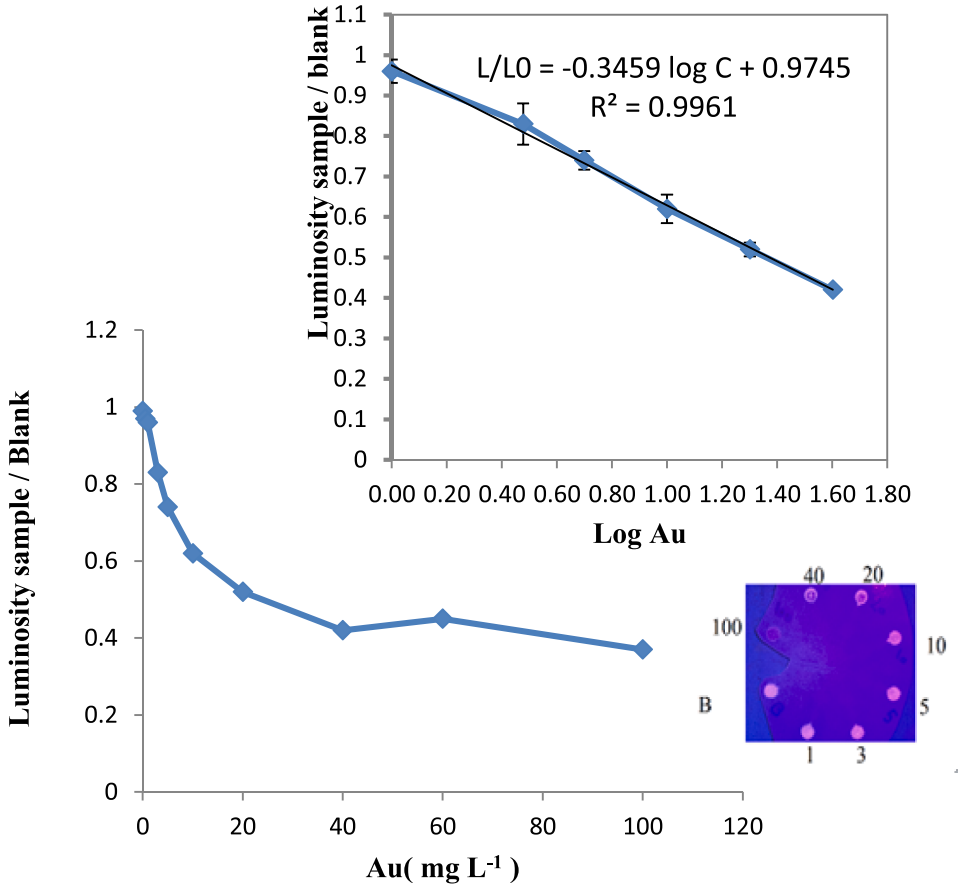

Fig. 3. Calibration curve under optimized conditions ([RB] = 0.187 mmol L^{-1}, pH = 3, [NaCl] = 40 mmol L^{-1}).Error bars represent the relative standard deviation of 3 times measurements.

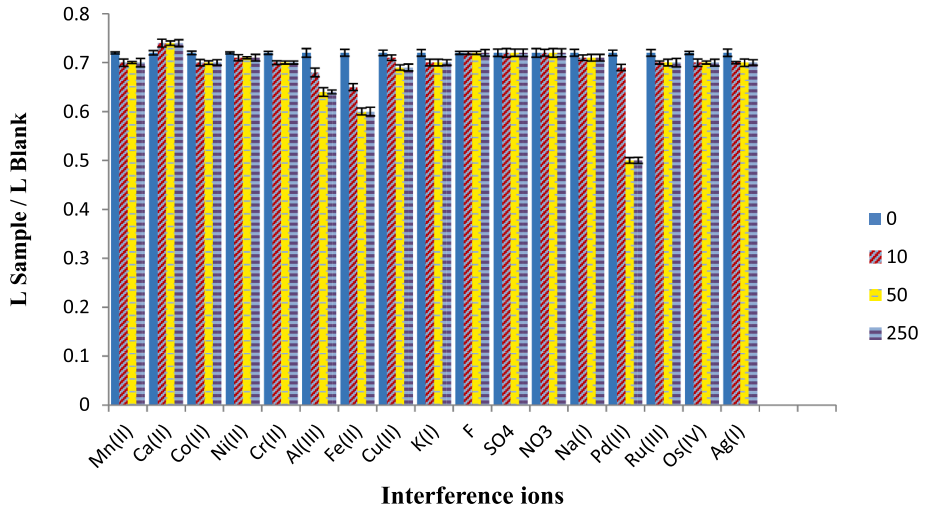

Fig. 4. The selectivity of μPAD for 20 mg L^{-1} gold in the presence of interferents at 10,50,250 mg L^{-1} (Ca(II),Cu(II),Al(III),Fe(III),Ni(II),Mn(II),Na(I),K(I),Cr(II),Co(II)Pd(II),Ru(II),Os(II), Ag(I), SO_4^{2-}, NO_3^-, PO_4^{3-}, F^-).

Table 1
Determination of gold in referenced standard materials.

NO	Code of CRM	Real Value (mg g^{-1})	Determined value by AAS (mg g^{-1})	Relative Error %	Determined value by this method (mg g^{-1})	Relative Error %
1	OXC129	0.205	*0.187 ± 0.007	8.78	0.213 ± 0.01	3.9
2	OREAS250	0.309	0.280 ± 0.05	9.3	0.289 ± 0.03	6.47
3	OXE106	0.606	0.63 ± 0.02	3.96	0.615 ± 0.04	1.48
4	SH82	1.333	1.35 ± 0.05	1.28	1.29 ± 0.06	3.22
5	OXJ95	2.337	2.22 ± 0.07	5.01	2.23 ± 0.08	4.58
6	OXL78	5.876	5.93 ± 0.09	0.92	5.68 ± 0.1	3.33

* Mean ± SD (N = 3).

which is equivalent to three times more than the standard deviation (SD) of luminosity for 8 blank samples, divided by regression line slop. The blank sample was prepared spotting with deionized water (pH = 3) in standard zones of μPAD.

3.4.2. Replicability of μPAD

The relative standard deviations were 4.3 and 1.4% for seven replicate analysis of 10 and 30 mg $L^{-1}Au^{3+}$, respectively. They indicated a good precision.

3.4.3. Selectivity

To evaluate the selectivity of the proposed sensor, different substances, which usually exist in gold ores, were tested at different concentrations of 10, 50 and 250mg L^{-1}. The results are represented in Fig. 4. No serious interference effect was observed in Ca(II), Cu(II), Ni (II), Mn(II), Na(I), K(I), Cr(II), Co(II), Ru(II), Os(II), Ag(I), SO_4^{2-}, NO_3^-, PO_4^{3-}, F^-. Fe (II), Pd(II) and Al (III), at concentrations greater than 10mg L^{-1}, had a positive interference effect. Meanwhile, as we know, in melting stage of fire assay, SiO_2, CaO, FeO, Al_2O_3, MgO, ZnO and other oxides go to slag [52]. Therefore, Fe (II) and Al (III) had no iterferencein gold determination. Palladium, as a precious metal, also does not exist in all ores.

3.4.4. Real samples analysis using of μPAD

To investigate the accuracy of the proposed method for real samples, six reference materials were selected and analyzed employing the proposed method. Analytical results and precision revealed (Table 1) that the data obtained by the proposed assay are in good agreement with the reference values. For the evaluation of the performance and applicability of this paper device in real geological samples, we used the μPAD to determine gold content in various gold ores of Zarmehr mine (Iran, Torbate heidarieh). Table 2 represents the obtained data. Paired *t*-test

Table 2
Determination of gold in real samples.

NO	Name of mine	Determined value by AAS (mg g^{-1})	Determined value by this method(mg g^{-1})
1	Ghare saleh (I)	*0.264 ± 0.01	0.260 ± 0.02
2	Gholleh khord	ND	0.028 ± 0.01
3	Talarearoos	0.83 ± 0.05	0.89 ± 0.07
4	Ghare kaftari	1.57 ± 0.02	1.51 ± 0.05
5	Ghare shahriar	10.4 ± 0.3	10.2 ± 0.4
6	Ghare kaftari	108 ± 2.4	112 ± 3.3

*Mean ± SD (N = 3).

analysis did not show any significant difference between the proposed assay and standard method with a confidence level of 95% [53]. To prepare a real sample, 50 g of the sample was weighed and melted. Coupling the fire assay method with μPAD led to the requirement of only low volume of samples (in usual method, final volume of sample is 10 mL, but in this work it was 2 mL) and because of three-times spotting of the samples, LOD decreased to 2 mg mL^{-1}, based on enrichment factor of 75.

3.4.5. Life time of the devices

For this purpose sensors were covered and stored at room temperature (25 °c ± 2) for up to 40 days after fabrication. Intensities as a function of storage time were shown in Fig. S7. These results show no significant color developed after 40 days to be useful for use in developing countries.

4. Conclusion

The proposed method showed that we could successfully combine high specificity fire assay preparation method with low-cost μPAD. This approach further benefits from a high sensitivity fluorescence detection with the aid of a smart phone. Fabricated μPAD demonstrated high precision, accuracy and sensitivity. This method reduced dependency on expensive equipment and is very suitable for small mines and industries, particularly in developing countries [54]. On detection zone of the μPAD, the reaction of gold obtained from fire assay of ore sample and rhodamine B triggered a decrease in fluorescence intensity of rhodamine B, which can be easily observed with naked eye. Quantitative analysis of gold was carried out using image analysis in Photoshop software. We are planning to develop the applicability of this μPAD for the determination of other precious metals in ores.

Declaration of Competing Interest

The authors declare that they have no known competing financial interests or personal relationships that could have appeared to influence the work reported in this paper.

Acknowledgment

The authors gratefully acknowledge the financial support of this research by Ferdowsi University of Mashhad, Mashhad, Iran.

Appendix A. Supplementary data

Supplementary data to this article can be found online at https://doi.org/10.1016/j.microc.2021.105923.

References

[1] Y. Rodríguez-Rodríguez, et al., Determination of Gold in Geological Samples Combining the Fire Assay and Ultraviolet Visible Spectrophotometry Techniques, 2018.
[2] A. Tunceli, A. Türker, Determination of gold in geological samples and anode slimes by atomic absorption spectrometry after preconcentration wth Amberlite XAD-16 resin, Analyst 122 (3) (1997) 239–242.
[3] M.R. Juvonen, et al., Comparison of Recoveries by Lead Fire Assay and Nickel Sulfide Fire Assay in the Determination of Gold/Platinum/Palladium and Rhenium in Sulfide Ore Samples, Geostand. Geoanal. Res. 28 (1) (2004) 123–130.
[4] M. El-Shahawi, A. Bashammakh, S. Bahaffi, Chemical speciation and recovery of gold (I, III) from wastewater and silver by liquid–liquid extraction with the ion-pair reagent amiloride mono hydrochloride and AAS determination, Talanta 72 (4) (2007) 1494–1499.
[5] I. De La Calle, et al., Ion pair-based dispersive liquid–liquid microextraction for gold determination at ppb level in solid samples after ultrasound-assisted extraction and in waters by electrothermal-atomic absorption spectrometry, Talanta 84 (1) (2011) 109–115.
[6] T. Itagaki, T. Ashino, K. Takada, Determination of trace amounts of gold and silver in high-purity iron and steel by electrothermal atomic absorption spectrometry after reductive coprecipitation, Fresenius' J. Anal. Chem. 368 (4) (2000) 344–349.
[7] R. Al-Merey, Z. Hariri, J.A. Hilal, Selective separation of gold from iron ore samples using ion exchange resin, Microchem. J. 75 (3) (2003) 169–177.
[8] R. Dobrowolski, et al., Determination of gold in geological materials by carbon slurry sampling graphite furnace atomic absorption spectrometry, Talanta 99 (2012) 750–757.
[9] D. Tao, et al., Rapid and accurate determination of gold in geological materials by an improved ICP-MS method, Microchem. J. 135 (2017) 221–225.
[10] Y. Hua, et al., Hybrid monolith assisted magnetic ion-imprinted polymer extraction coupled with ICP-MS for determination of trace Au (III) in environmental and mineral samples, Microchem. J. (2020).
[11] A.V. Volzhenin, et al., Multiple probe concentrating of Au and Pd in geological samples for atomic absorption determination with two-stage probe atomization, Microchem. J. 138 (2018) 390–394.
[12] W. Ni, et al., Simultaneous determination of ultra-trace Au, Pt, Pd, Ru, Rh, Os and Ir in geochemical samples by KED-ICP-MS combined with Sb-Cu fire assay and microwave digestion, Microchem. J. (2020) 105197.
[13] A.W. Martinez, et al., Diagnostics for the developing world: microfluidic paper-based analytical devices, ACS Publications, 2009.
[14] P.J. Bracher, M. Gupta, G.M. Whitesides, Patterning precipitates of reactions in paper, J. Mater. Chem. 20 (24) (2010) 5117–5122.
[15] T. Kaneta, W. Alahmad, P. Varanusupakul, Microfluidic paper-based analytical devices with instrument-free detection and miniaturized portable detectors, Appl. Spectrosc. Rev. 54 (2) (2019) 117–141.
[16] C.-K. Chiang, et al., Single step and mask-free 3D wax printing of microfluidic paper-based analytical devices for glucose and nitrite assays, Talanta 194 (2019) 837–845.
[17] H. Wang, et al., Based three-dimensional microfluidic device for monitoring of heavy metals with a camera cell phone, Anal. Bioanal. Chem. 406 (12) (2014) 2799–2807.
[18] T. Songjaroen, et al., Blood separation on microfluidic paper-based analytical devices, Lab Chip 12 (18) (2012) 3392–3398.
[19] Y. Lu, et al., Rapid prototyping of paper-based microfluidics with wax for low-cost, portable bioassay, Electrophoresis 30 (9) (2009) 1497–1500.
[20] E. Carrilho, A.W. Martinez, G.M. Whitesides, Understanding wax printing: a simple micropatterning process for paper-based microfluidics, Anal. Chem. 81 (16) (2009) 7091–7095.
[21] K. Yamada, et al., Paper-based inkjet-printed microfluidic analytical devices, Angew. Chem. Int. Ed. 54 (18) (2015) 5294–5310.
[22] A.W. Martinez, et al., Patterned paper as a platform for inexpensive, low-volume, portable bioassays, Angew. Chem. Int. Ed. 46 (8) (2007) 1318–1320.
[23] A.W. Martinez, et al., Simple telemedicine for developing regions: camera phones and paper-based microfluidic devices for real-time, off-site diagnosis, Anal. Chem. 80 (10) (2008) 3699–3707.
[24] X. Li, et al., Based microfluidic devices by plasma treatment, Anal. Chem. 80 (23) (2008) 9131–9134.
[25] P. Spicar-Mihalic, et al., CO2 laser cutting and ablative etching for the fabrication of paper-based devices, J. Micromech. Microeng. 23 (6) (2013).
[26] J. Wang, et al., Hydrophobic sol–gel channel patterning strategies for paper-based microfluidics, Lab Chip 14 (4) (2014) 691–695.
[27] Y. Zhang, et al., Hydrophobic/lipophobic barrier capable of confining aggressive liquids for paper-based assay, Colloids Surf., A 520 (2017) 544–549.
[28] W. Dungchai, O. Chailapakul, C.S. Henry, A low-cost, simple, and rapid fabrication method for paper-based microfluidics using wax screen-printing, Analyst 136 (1) (2011) 77–82.
[29] G. Sriram, et al., Based microfluidic analytical devices for colorimetric detection of toxic ions: A review, TrAC, Trends Anal. Chem. 93 (2017) 212–227.
[30] D. Lin, et al., Low cost fabrication of microfluidic paper-based analytical devices with water-based polyurethane acrylate and their application for bacterial detection, Sens. Actuators, B 303 (2020).
[31] L. Xie, et al., Low-cost fabrication of a paper-based microfluidic using a folded pattern paper, Anal. Chim. Acta 1053 (2019) 131–138.
[32] G.G. Morbioli, et al., Technical aspects and challenges of colorimetric detection with microfluidic paper-based analytical devices (μPADs)-A review, Anal. Chim. Acta 970 (2017) 1–22.
[33] J. Mettakoonpitak, et al., Electrochemistry on paper-based analytical devices: a review, Electroanalysis 28 (7) (2016) 1420–1436.
[34] J.-M. Oh, K.-F. Chow, Recent developments in electrochemical paper-based analytical devices, Anal. Methods 7 (19) (2015) 7951–7960.
[35] K. Scida, et al., DNA detection using origami paper analytical devices, Anal. Chem. 85 (20) (2013) 9713–9720.
[36] R.V. Taudte, et al., A portable explosive detector based on fluorescence quenching of pyrene deposited on coloured wax-printed μPADs, Lab Chip 13 (21) (2013) 4164–4172.
[37] L. Ge, et al., Lab-on-paper-based devices using chemiluminescence and electrogenerated chemiluminescence detection, Anal. Bioanal. Chem. 406 (23) (2014) 5613–5630.
[38] F. Li, et al., Multiplexed chemiluminescence determination of three acute myocardial infarction biomarkers based on microfluidic paper-based immunodevice dual amplified by multifunctionalized gold nanoparticles, Talanta 207 (2020).
[39] E.M. Gross, et al., Electrochemiluminescence detection in paper-based and other inexpensive microfluidic devices, ChemElectroChem 4 (7) (2017) 1594–1603.
[40] S.R. Chinnadayyala, et al., Recent advances in microfluidic paper-based electrochemiluminescence analytical devices for point-of-care testing applications, Biosens. Bioelectron. 126 (2019) 68–81.
[41] D.D. Liana, et al., Recent advances in paper-based sensors, Sensors 12 (9) (2012) 11505–11526.
[42] M. He, et al., Portable upconversion nanoparticles-based paper device for field testing of drug abuse, Anal. Chem. 88 (3) (2016) 1530–1534.
[43] M.-M. Liu, et al., A colorimetric assay for sensitive detection of hydrogen peroxide and glucose in microfluidic paper-based analytical devices integrated with starch-iodide-gelatin system, Talanta 200 (2019) 511–517.
[44] M.A. Ostad, A. Hajinia, T. Heidari, A novel direct and cost effective method for fabricating paper-based microfluidic device by commercial eye pencil and its application for determining simultaneous calcium and magnesium, Microchem. J. 133 (2017) 545–550.
[45] P. Battaini, E. Bemporad, D. De Felicis, The fire assay reloaded, Gold Bull. 47 (1–2) (2014) 9–20.
[46] A. Nilghaz, X. Lu, Detection of antibiotic residues in pork using paper-based microfluidic device coupled with filtration and concentration, Anal. Chim. Acta 1046 (2019) 163–169.
[47] Q.-J. Ma, et al., A highly selective fluorescent probe for Hg2+ based on a rhodamine–coumarin conjugate, Anal. Chim. Acta 663 (1) (2010) 85–90.
[48] J.Fries, H.G., Organic reagents for trace analysis, 1977.

[49] E. Evans, et al., Rational selection of substrates to improve color intensity and uniformity on microfluidic paper-based analytical devices, Analyst 139 (9) (2014) 2127–2132.
[50] Z. Marczenko, M. Balcerzak, Separation, preconcentration and spectrophotometry in inorganic analysis. 2000: Elsevier.
[51] I. Mironov, E. Makotchenko, The Hydrolysis of AuCl 4− and the Stability of Aquachlorohydroxocomplexes of Gold (III) in Aqueous Solution, J. Solution Chem. 38 (6) (2009) 725–737.
[52] D. Flaxbart, Kirk− Othmer Encyclopedia of Chemical Technology, 27-Volume Set Wiley Interscience: New York, 1992− 1998. $7884. ISBN 0-471-52704-1. 1999, ACS Publications.
[53] J. Miller, J.C. Miller, Statistics and chemometrics for analytical chemistry. 2018: Pearson education.
[54] Y. Wang, et al., Label-free microfluidic paper-based electrochemical aptasensor for ultrasensitive and simultaneous multiplexed detection of cancer biomarkers, Biosens. Bioelectron. 136 (2019) 84–90.